Surface Characterization of Nanoscale TiO_2 Film by Sum Frequency Generation Using Methanol as a Molecular Probe

Chuan-yi Wang, Henning Groenzin, and Mary Jane Shultz*

Department of Chemistry, Pearson Laboratory, Tufts University, Medford, Massachusetts 02155

Received: June 10, 2003; In Final Form: October 20, 2003

Sum frequency generation (SFG) vibrational spectroscopy is applied to study the surface characteristics of a film composed of nanoscale TiO_2 particles, in which methanol is employed as a molecular probe. The SFG signal from methanol adsorbed on the TiO_2 film surface in the CH region consists of four primary peaks located at 2828, 2855, 2935, and 2968 cm^{-1}. The peaks at 2855 and 2968 cm^{-1} arise from molecular methanol; the other two are attributed to methoxy produced by dissociative chemisorption of methanol on TiO_2. Changes in the SFG features with methanol pressure and with surface temperature provide the first direct proof of methoxy generation on nanoparticulate films. In comparison with molecular methanol, methoxy sits more perpendicularly on the surface. The chemisorption is barrierless, and a Langmuir constant of $(2.13 \pm 0.14) \times 10^3$ is derived from the adsorption isotherm. Moreover, UV pretreatment of the TiO_2 film substantially increases the methoxy signal. Changes in SFG intensity are in good agreement with the current models for surface active sites and face specificities on TiO_2.

1. Introduction

Titanium dioxide, TiO_2, is a versatile material with important applications in many fields, particularly in environmental purification and energy storage and transfer.[1−7] Recently, Wang et al.[4,8,9] reported reversible wettability of TiO_2 with UV irradiation. This property is attractive for the application of TiO_2 to a variety of environments. Although the chemical mechanisms of TiO_2 vary in detail for different applications, the basic processes all occur on its surface. In an effort to identify the surface sites and mechanisms, many experiments have been carried out by a variety of techniques including X-ray photoelectron microscopy (XPS),[10,11] atomic force microscopy (AFM),[12] Fourier transform infrared spectroscopy (FTIR),[10,13,14] Raman spectroscopy,[15,16] and high-resolution electron-energy-loss spectroscopy (HREELS).[17,18] Important results have been obtained with these techniques but they are limited in their applicability. Specifically, these techniques are either not surface-sensitive at a molecular level (FTIR, Raman), require an ultrahigh vacuum (UHV) environment (XPS, HREELS), or cannot distinguish among molecular species on nanoparticulate surfaces (AFM). In contrast, sum frequency generation (SFG) spectroscopy has been shown to be an effective surface/interface probe.[19−28]

In the field of molecular spectroscopy, methanol has been referred to as the most complicated simple molecule.[29] It consists of only five atoms, but its molecular symmetry is very low, belonging to the C_s point group. Furthermore, molecular methanol contains hydroxyl as an active group, making it suitable as a molecular surface probe for many metal oxides.

There are a number of reports about the adsorption of methanol on TiO_2. On the basis of ultraviolet photoelectron spectroscopy (UPS) results, Onishi et al.[30] report that methanol adsorbs in a molecular state on the stoichiometric (110) and (441) surfaces of a rutile single crystal. Yet Ramis et al.[31] concluded that the adsorption is dissociative as evidenced by IR measurements on a self-supporting disk of powdered rutile. Temperature-programmed desorption (TPD) and UPS studies on (001) rutile single-crystal surfaces by Kim and Barteau[32] show that dissociative adsorption predominates on the stoichiometric surface, while both dissociative and molecular adsorption modes coexist on the reduced surface. On the basis of theoretical simulations, Bates et al.[33] concluded that there are several different adsorption conformations for methanol on rutile TiO_2 (110). Simulations indicate that both molecular and dissociative adsorptions are within a narrow energy range. A very recent study of TPD and XPS on anatase−TiO_2 (101) by Herman et al.[34] also verifies both molecular and dissociative adsorption modes. From the published literature one has to draw the conclusion that the adsorption of methanol on TiO_2 varies from face to face and sample to sample. Although the adsorption of methanol on TiO_2 has been extensively studied in recent decades, it is not yet well understood. Open issues include the orientation or site for methanol versus methoxy adsorption and how surface treatment, i.e., UV irradiation, affects the adsorption.

Methanol also serves an important role in TiO_2 photocatalysis as a scavenger of photogenerated holes and as a probe to determine the quantum yield of hydroxyl radicals for evaluation of the photocatalytic activity of the material.[35−37] Many applications, e.g., photocatalysis and solar cells, involve TiO_2 in powdered, colloidal, and/or polycrystalline form (mainly anatase). However, most of the previous studies were performed on single crystals of rutile. Therefore, it is of interest to obtain information about methanol adsorption directly on colloidal and polycrystalline anatase samples.

In the present work, methanol is used as a molecular probe of a nanoparticulate TiO_2 film surface. The SFG spectrum of methanol on TiO_2 is obtained for the first time. The dependence of the SFG intensity on (1) methanol pressure, (2) surface temperature, (3) polarization combinations, and (4) UV treatment of the TiO_2 film is presented. Surface adsorption modes, molecular orientation on the surface, and surface active sites

* To whom correspondence should be addressed: Tel 617 627 4810; fax 617 627 3443; e-mail Mary.Shultz@tufts.edu.

10.1021/jp0356463 CCC: $27.50
Published on Web 11/27/2003

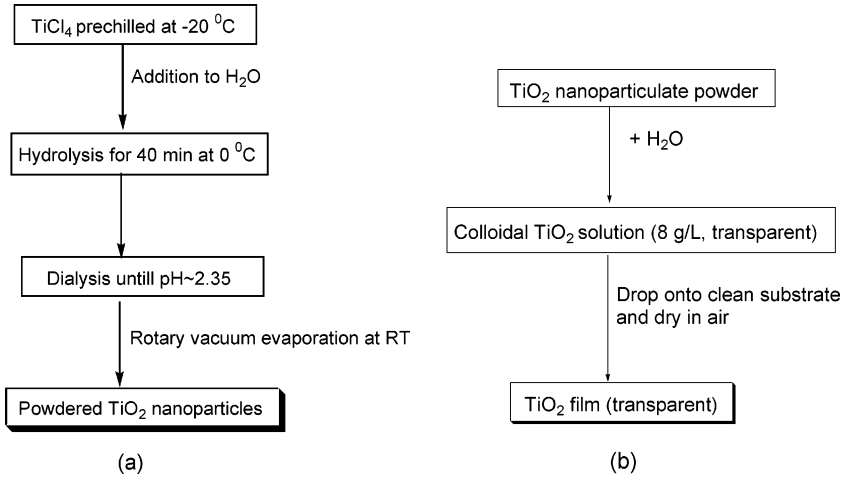

Figure 1. Preparation of TiO_2 nanoparticles (a) and nanoparticulate film (b).

are thereby probed. The SFG signal from methanol on TiO_2 is found to be sensitive to surface treatment. Changes in SFG spectrum due to the varying conditions reflect the nature of active sites on the surface of TiO_2.

The probe technique, SFG, is a second order, $\chi^{(2)}$, process, and within the electric dipole approximation it occurs only in environments without inversion symmetry. As an optical spectroscopy, SFG can be used in any environment that is accessible to the visible and infrared beams. Being a vibrational spectroscopy, SFG is specific to the species and their environment. The SFG intensity, I_{SF}, is proportional to the square of the second-order nonlinear susceptibility, $\chi_{IJK}^{(2)}$:

$$I_{SF} \propto \left(\sum \chi_{IJK}^{(2)} L_{sum} K_{vis} K_{IR} E_{vis} E_{IR}\right)^2 \quad (1)$$

where *I*, *J*, *K* is the surface coordinate system, *E* represents the electric fields at the surface, and *K* and *L* are the linear and nonlinear Fresnel coefficients, respectively. The second-order nonlinear susceptibility can be decomposed into a nonresonant term and a resonant term:

$$\chi^{(2)} = \chi_{NR}^{(2)} + \chi_{R}^{(2)} \quad (2)$$

The resonant term $\chi_R^{(2)}$ depends on the density of the molecules (N) on the surface and the molecular hyperpolarizability (β) averaged over all molecular orientations on the surface:

$$\chi_{R}^{(2)} = N\langle\beta\rangle/\epsilon_0 \quad (3)$$

where ϵ_0 is the permittivity of free space. Within the electric dipole approximation, β can be expressed as[38,39]

$$\beta_{q,lmn} = \frac{\alpha_{q,lm}\mu_{q,n}}{2\hbar(\omega_q - \omega_{IR} - i\Gamma_q)} \quad (4)$$

where $\alpha_{q,lm}$, $\mu_{q,n}$, ω_q, ω_{IR}, and Γ_q are the Raman tensor element, IR transition dipole moment, resonant frequency, frequency of IR beam, and the damping constant of the qth molecular vibrational mode, respectively. These basic SFG principles, eqs 2−4, are often used to fit the SFG spectrum and extract information about the mode strength and peak position.

2. Experimental Section

The process for the preparation of TiO_2 nanoparticles and fabrication of them into films is schematically illustrated in Figure 1.

As shown by regular and high-resolution transmission electron microscopy (TEM and HRTEM), the average size of the prepared TiO_2 particles is ca. 2.4 nm with a crystal structure of anatase. The films used in this work are ca. 500 nm thick, as determined by a profilometer (Sloan DEK TAK). UV irradiation to clean the surface of the TiO_2 film when necessary is achieved by means of a 1000 W ozone-free Xe lamp (Oriel Instruments) equipped with a 10-cm water filter to eliminate IR radiative heating.

The TiO_2 film deposited on a CaF_2 substrate was mounted on a vacuum cell for the SFG experiments. SFG is accomplished by temporally and spatially overlapping a 532 nm visible and a tunable IR beam on the TiO_2 film surface at incident angles of 50° and 60°, respectively, relative to the surface normal. The detailed system producing the visible and tunable IR beams has been reported elsewhere.[40] The SFG signal from the sample surface is collected in reflection by a photomultiplier tube after filtration by a polarizer and monochromator. The IR input energy is monitored during the experiment by an energy meter (Molectron J8LP + ENERGY MAX500). The vibrational spectrum from the surface is normalized to the input beam intensities and referenced to the signal from silver. Each data point, taken at a resolution of 4 cm^{-1}, is averaged over 3000 pulses with a gated integrator (Stanford Research Systems, SR250) and stored in a personal computer.

3. Results and Discussion

3.1. UV−Vis Absorption Spectroscopy and AFM Characterizations. Figure 2 shows the absorption spectra of a TiO_2 film on CaF_2 and the colloidal seed solution. The seeded colloidal TiO_2 solution is clear with virtually no scattering, and the formed film is optically transparent. The corresponding band gaps of the TiO_2 film and the seeded colloidal particles evaluated by the absorption onsets are 3.26 and 3.51 eV, respectively. The increased band gap for colloidal TiO_2 arises from quantum confinement. When the size of the semiconductor particles is comparable to or smaller than the de Broglie wavelength of the exciton, the density of electronic states decreases and the allowed energy states become discrete rather than continuous. Brus[41] calculated the electronic wave functions in semiconductor clusters and derived a formula for the radius α of an exciton:

$$\alpha = \frac{\epsilon}{m_e^*/m_e} a_0 \quad (5)$$

where a_0 is the hydrogen Bohr radius, 0.53 Å; ϵ is the dielectric

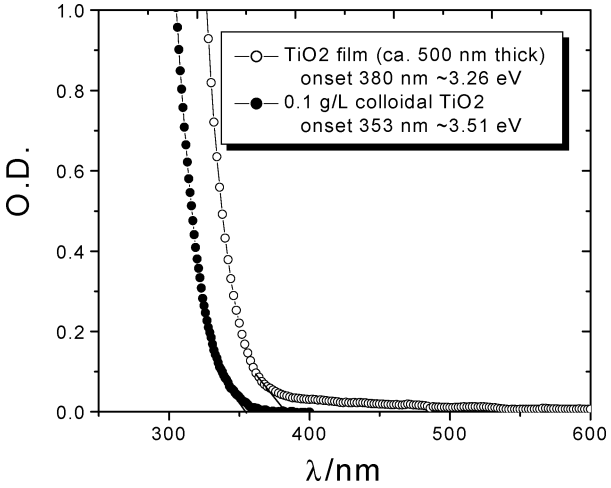

Figure 2. UV−Vis spectra of colloidal TiO_2 solution and nanoparticulate film.

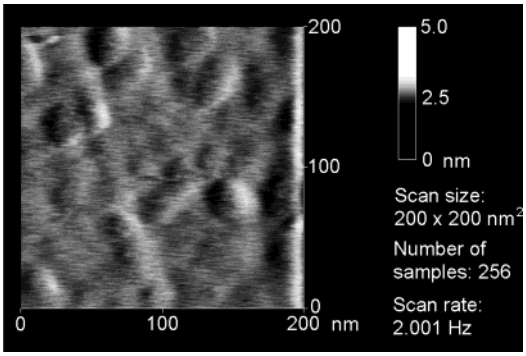

Figure 3. AFM image of a TiO_2 film on CaF_2.

constant; and m_e* is the effective mass of the electron. According to the Brus formula, the exciton radius for TiO_2 is between 7.5 and 19 Å as calculated by Kormann et al.[42] The average radius of the colloidal TiO_2 used in the present work is ca. 1.2 nm, as measured by TEM, and falls within this range. There is controversy in the literature about whether nanometer-sized TiO_2 particles exhibit quantum effects.[43] However, a shift in the absorption band edge in Figure 2 is apparent.

The band gap of the TiO_2 film is smaller than that of the colloidal solution and is comparable to that of bulk anatase TiO_2 ($E_g \sim 3.25$ eV). Aggregation of the primary particles is expected to occur during film formation. This conclusion is confirmed by AFM measurements. Figure 3 shows that the particles of the film are ca. 20 nm in diameter. On a macroscopic scale, the film surface is flat with a RMS (root-mean-square) roughness of ±0.5 nm, enabling efficient collection of the SFG signal.

The TiO_2 film is grown "bottom-up" on a substrate. Isotropic symmetry is broken at the top layer of the film, which is open to methanol molecules in the vapor phase on the gas-phase side and embedded in the film on the film side. The interior of the film can be regarded as a bulk phase. Molecular species, like methanol, that penetrate into the film wherein isotropic symmetry exists do not contribute to the SFG signal. Adsorbed molecules are randomly oriented in the plane perpendicular to the surface normal. Due to the asymmetric environment, molecules adopt a preferred polar orientation along the surface normal. This preferred orientation gives rise to the SFG signal.

3.2. SFG Spectral Features of Methanol on TiO_2. Figure 4 shows the SFG spectrum of methanol at the neat liquid/air interface. There are two primary peaks located at 2849 and 2965 cm^{-1} assigned to the symmetric (ν_s) and asymmetric (ν_{as})

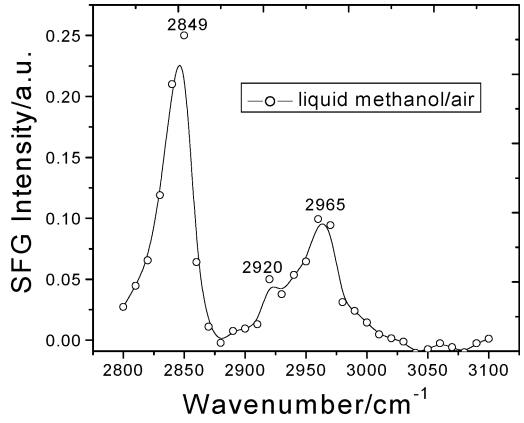

Figure 4. SFG spectrum of the neat methanol liquid/air interface (*ssp*-polarization combination).

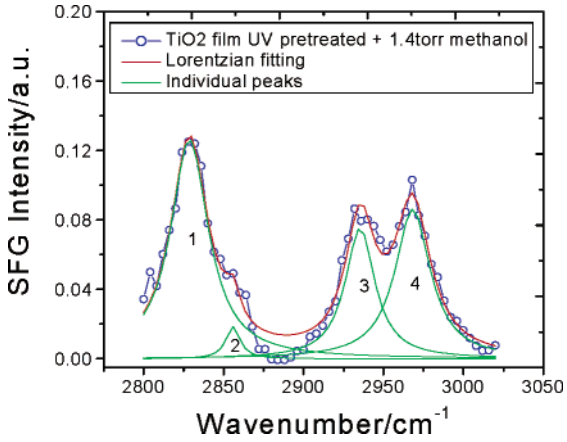

Figure 5. SFG spectrum of methanol on a TiO_2 film (*ssp*-polarization combination).

stretch, respectively. In addition, there is a shoulder around 2920 cm^{-1}, assigned to the Fermi resonance of the CH_3 ν_s stretching mode with the overtone of the CH_3 bending mode. The spectral features are consistent with previously reported results.[44−46]

A typical SFG spectrum of methanol on a TiO_2 film is shown in Figure 5. To the best of our knowledge, this is the first SFG spectrum of methanol adsorbed on a metal oxide surface. As seen in Figure 5, the baseline of the spectrum is very close to zero, indicating that the nonresonant contribution to the SFG signal from the TiO_2 semiconductor substrate is negligibly small, i.e., the term $\chi_{NR}^{(2)}$ in eq 2 is ~0. According to eqs 1−4, the spectrum of Figure 5 is fitted by a Lorentzian line shape with four resonant peaks at positions 2828, 2855, 2935, and 2968 cm^{-1}, respectively.

By comparison with the SFG spectrum from pure methanol (Figure 4), the two peaks at 2855 and 2968 cm^{-1} in Figure 5 are assigned to the symmetric and asymmetric vibrational modes of molecular methanol on TiO_2. It is interesting to note that the intensity ratio between the two peaks for molecular methanol on the TiO_2 surface is dramatically different from that at the liquid/air interface, reflecting the different molecular orientations (discussed below).

On the basis of FTIR studies,[47] the other two peaks located at 2828 and 2935 cm^{-1} (Figure 5) are assigned to methoxy, a product of chemisorption of methanol on TiO_2. Although assignment of these peaks to methoxy can be found in a number of papers, proof has been tenuous. For the first time, experimental support for this assignment is provided by the change of the SFG signal with both pressure (Figure 6) and temperature (Figure 7).

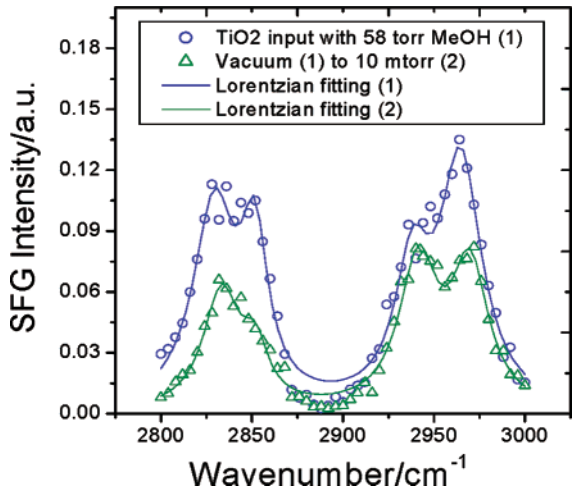

Figure 6. Effect of methanol pressure reduction on SFG intensity.

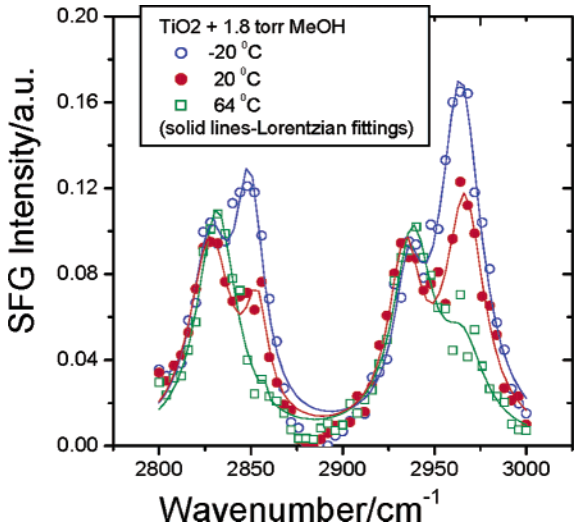

Figure 7. Effect of the change in surface temperature on SFG intensity of methanol on TiO_2.

When the system is evacuated (Figure 6) or heated (Figure 7), the SFG resonances arising from molecular methanol are greatly decreased while the other two peaks are little affected. The two peaks insensitive to pressure and temperature arise from a species that is strongly adsorbed on TiO_2, i.e., methoxy. The evidence put forth supports a model wherein gaseous methanol impinges upon the TiO_2 film surface interacting by two types of surface adsorption: chemisorption and physisorption. The two adsorption modes result in two species on the surface: methoxy and methanol. This is in keeping with previously reported results on powdered TiO_2 samples.[48] In addition, a recent report in which UHV was used to probe methanol interaction with single-crystal anatase (101) is consistent with both molecular adsorption and dissociative adsorption leading to methoxy.[34]

3.3. Orientation of Methanol on TiO_2. A significant advantage of SFG studies is the capability to determine molecular orientation. In general, the molecular orientation is determined by comparing SFG intensities from different polarization combinations. Figure 8 shows the SFG intensities at the four peak positions with various polarization combinations. As has become standard in the field, the first letter refers to the polarization of the emitted SFG light, the second to the incident visible beam, and the third to the input IR beam.

As seen in Figure 8, the signal from methoxy (peaks 1 and 3) has a different dependence on polarization than that from

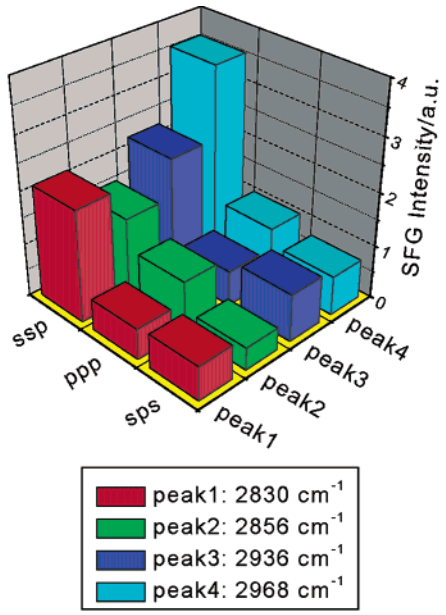

Figure 8. Peak SFG intensities for the three unique nonzero polarization combinations.

molecular methanol. Relatively speaking, the signal for both species is most intense for the *ssp* combination, while the *ppp* signal is more intense for molecular methanol than methoxy, and the *sps* signal is more intense for methoxy than molecular methanol. This indicates that these two species, methoxy and methanol, adsorb on the surface in very different orientations.

In the case of an azimuthally isotropic interface, the second-order nonlinear susceptibility has only three independent, nonzero components so only three contribute to the SFG signal of methanol or methoxy on the TiO_2 film. The relationship between the second-order nonlinear susceptibility components and the molecular hyperpolarizability tensor elements are available in the literature.[38,49−52] In keeping with usual practice,[38,49−52] the methyl groups of both methanol and methoxy are treated as having C_{3v} symmetry, although the molecular symmetry may be lower. For C_{3v}, there are only two nonvanishing independent elements in the symmetric stretch hyperpolarizability tensor: β_{ccc} and $\beta_{aac} = \beta_{bbc}$. The antisymmetric stretch hyperpolarizability tensor has only one independent element: β_{caa}. For the symmetric stretch the components of χ are given by

$$\chi_{xxz,s} = \chi_{yyz,s} = \frac{1}{2}N_s\beta_{ccc}[(1+r)\cos\theta - (1-r)\cos^3\theta] \quad (6a)$$

$$\chi_{xzx,s} = \chi_{yzy,s} = \chi_{zxx,s} = \chi_{zyy,s} = \frac{1}{2}N_s\beta_{ccc}(1-r)[\cos\theta - \cos^3\theta] \quad (6b)$$

$$\chi_{zzz,s} = N_s\beta_{ccc}[r\cos\theta + (1-r)\cos^3\theta] \quad (6c)$$

where $r = \beta_{aac}/\beta_{ccc}$ and θ is the polar angle of the symmetry axis c with respect to the surface normal z; a δ-function for the angular distribution of the adsorbed molecules is assumed. For the antisymmetric stretch, the components of χ can be expressed as

$$\chi_{xxz,as} = \chi_{yyz,as} = -N_s\beta_{caa}(\cos\theta - \cos^3\theta) \quad (7a)$$

$$\chi_{xzx,as} = \chi_{yzy,as} = \chi_{zxx,as} = \chi_{zyy,as} = \beta_{caa}N_s\cos^3\theta \quad (7b)$$

$$\chi_{zzz,as} = 2N_s\beta_{caa}(\cos\theta - \cos^3\theta) \quad (7c)$$

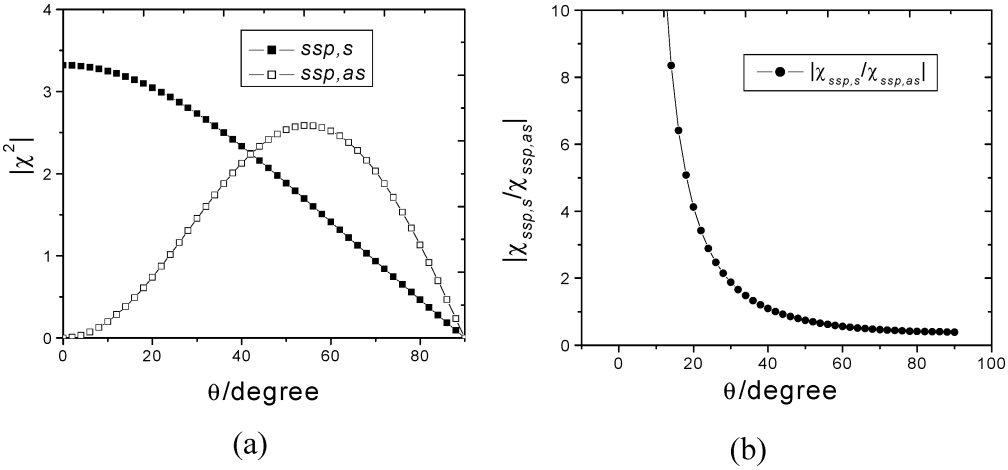

Figure 9. SFG intensities for the symmetric and asymmetric stretch of methyl (a) and the ratio between them (b) as a function of tilt angle.

Since $\beta_{q,lmn} \propto \alpha_{q,lm}\mu_{q,n}$ (cf. eq 5), $r = \beta_{aac}/\beta_{ccc} = \alpha_{aa}/\alpha_{cc}$. The ratio, r, of Raman polarizability elements is related to the Raman depolarization ratio as follows.[53] The depolarization ratio, $\rho = I_\perp/I_{||}$, is given by

$$\rho = \frac{3g^s + 5g^a}{10g^0 + 4g^s} \tag{8}$$

where

$$g^0 = \frac{1}{3}(\alpha_{xx} + \alpha_{yy} + \alpha_{zz})^2$$

$$g^s = \frac{1}{3}[(\alpha_{xx} - \alpha_{yy})^2 + (\alpha_{yy} - \alpha_{zz})^2 + (\alpha_{zz} - \alpha_{xx})^2] + \frac{1}{2}[(\alpha_{xy} + \alpha_{yx})^2 + (\alpha_{yz} + \alpha_{zy})^2 + (\alpha_{xz} + \alpha_{zx})^2]$$

$$g^a = \frac{1}{2}[(\alpha_{xy} - \alpha_{yx})^2 + (\alpha_{yz} - \alpha_{zy})^2 + (\alpha_{xz} - \alpha_{zx})^2]$$

Thus, the anisotropy of the hyperpolarizability ellipsoid, i.e., the ratio r, is related to the experimental Raman depolarization ratio ρ.[54,55] On the basis of the experimental value $\rho = 0.014$ for the symmetric stretch vibration of the methyl group of methanol,[56] the ratio r is calculated to be 1.66. This is in the reasonable range of 1.5−4.2 for methyl group as reported by Zhuang et al.[50]

For the antisymmetric stretch, as is seen from eq 7, the components of χ are related to only one independent element, β_{caa}. To compare the relative SFG intensity of the antisymmetric stretch with the symmetric stretch, a ratio of β_{caa}/β_{aac} or β_{caa}/β_{ccc} is required. The former value is estimated as follows. Theoretical calculations of the hyperpolarizabilities of hydrocarbons show that the group polarizabilities are transferable.[57] Watanabe et al.[51] estimated a value of $\beta_{caa}/\beta_{aac} = 4.2$ for the antisymmetric vibrational stretching band of the methyl group of cadmium arachidate. The value is adopted here.

For the *ssp* polarization combination, the dependence of the second-order susceptibilities on the tilt angle, shown in Figure 9, is based on a random CH_3 twist angle. The experimental data shown in Figure 5 and 8 indicate that the average tilt angles for methoxy and methanol on the TiO_2 film surface are significantly different. If a δ-function tilt angle distribution is assumed, the tilt is derived to be about 35° and 70°, respectively. The broader angular distribution results in an uncertainty in the tilt angle of ±10°.[51]

It should be understood that the angles given here are measured with respect to the "optical surface normal". The flatness of the surface of the TiO_2 film, addressed previously, is sufficient to create a specular reflection (as opposed to a diffuse reflection) of the SFG beam. This is easily shown by a HeNe laser beam following the exit angle of the SFG beam. The reflection of the optical beams then defines an optical surface normal with respect to which the orientation of the adsorbate is measured. Since the surface of the TiO_2 is not flat on the atomic level (RMS roughness of ±0.5 nm over 200 nm; see Figure 3) it is clear that the absolute angle of the adsorbate with respect to the atomic-scale surface structure is not determined by this experiment, since the atomic-scale surface normal is unknown. The angle with respect to the "optical surface normal" represents an average over the molecular orientations. Since the surface is the same for molecular methanol and methoxy, both species are affected equally by the "optical averaging". Their relative angle remains meaningful. A schematic of methanol and methoxy on a TiO_2 film optical surface is shown in Figure 10. The symmetry axis of the CH_3 group of methanol lies more flat to the surface than does the same axis of the methoxy species. The conclusion based on polarization measurements is strengthened by the higher intensity of the asymmetric stretch mode of molecular methanol compared to the symmetric stretch mode.

The spectral features of molecular methanol at liquid/air interface and on the TiO_2 film surface (Figures 4 and 5) are dramatically different, indicating a difference in the molecular orientations on these two surfaces. From Figure 4, the average tilt angle of molecular methanol at the neat liquid/air interface is in the range of 20−30°. This agrees well with the prediction of $\theta = 23°$ from computational simulations.[58] Interaction with the TiO_2 surface results in an orientation with the methyl group C_3 axis more parallel to the surface than that for neat methanol. Since the *ssp* polarization intensity reflects the projection of the transition dipole on the surface normal, the increased tilt angle relative to neat methanol increases the antisymmetric stretch intensity relative to that of the symmetric stretch.

3.4. Nature of Adsorption and Implications for Surface Site Characteristics: 3.4.1. Chemisorption Isotherm. Chemisorption is closely related to the number and nature of the surface active sites. In the present work, the surface active sites can be quantitatively evaluated from the SFG signal due to methoxy, which can be abstracted from spectral data fitting as shown in Figure 5. The resonant SFG signal intensity is proportional to the square of the number of molecules contributing to the signal

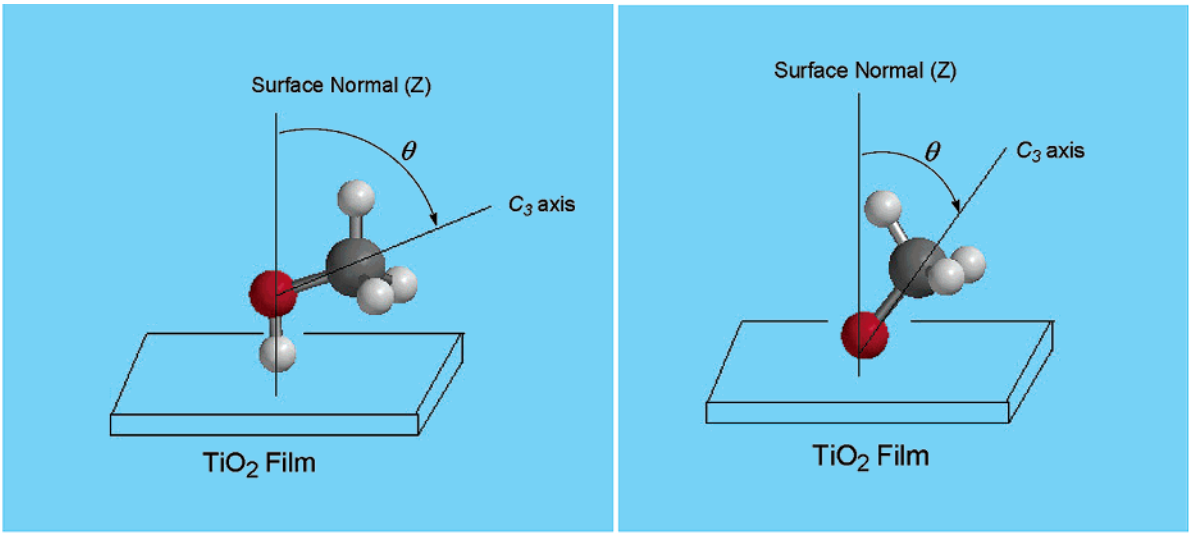

Figure 10. Adsorption of methanol and methoxy on a TiO_2 film surface (red, oxygen; white, hydrogen; black, carbon).

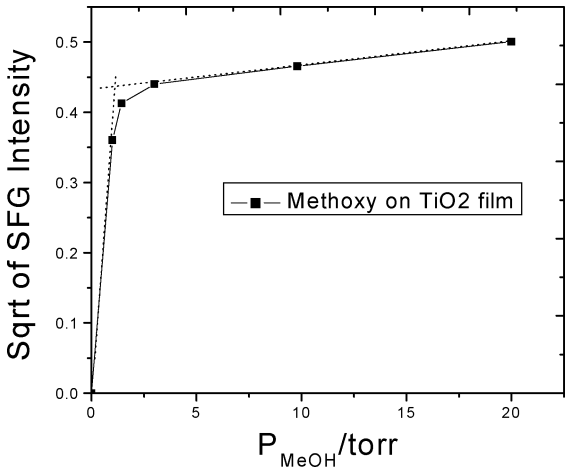

Figure 11. Square root of methoxy on TiO_2 SFG intensity vs methanol pressure (RT).

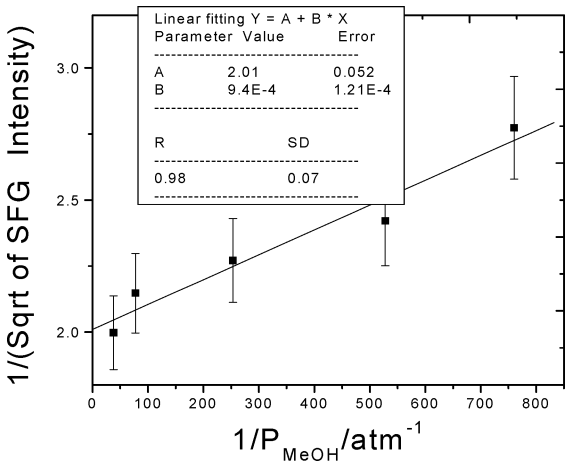

Figure 12. Relationship between the inverse square root of the methoxy on TiO_2 SFG intensity and the inverse methanol pressure.

(eqs 3 and 4) and to their average orientation:

$$I_{SF} \propto |\chi^{(2)}|^2 = N^2|\langle\beta\rangle|^2 \tag{9}$$

An adsorption isotherm can thus be obtained by following the SFG intensities of methoxy at various methanol pressures (Figure 11, room temperature). Up to ~1 Torr, the surface coverage shows a monotonic dependence on the pressure of methanol in the gas phase and suggests that multilayer adsorption is not occurring to a measurable extent. A knee appears at a pressure of ca. 1 Torr in Figure 11, indicating formation of a monolayer. This inflection point reflects the density of active sites available on the surface. The plateau at higher pressure signifies the approach to surface saturation. The general shape of the curve suggests a Langmuir adsorption mode.

A Langmuir mode of gas adsorbed on a solid surface obeys[59]

$$\theta = \frac{N}{N_{max}} = \frac{K(T)P}{1 + K(T)P} \tag{10}$$

where θ is the fractional surface coverage, N is the molecular coverage or density as defined previously (molecules per square centimeter), N_{max} is the molecular coverage at saturation, $K(T)$ is the temperature-dependent Langmuir adsorption constant that describes partitioning between molecules in the gas phase and those adsorbed on the surface, and P is the vapor pressure of the adsorbate. Inverting eq 10, one obtains

$$\frac{1}{N} = \frac{1}{N_{max}} + \frac{1}{N_{max}K(T)}\left(\frac{1}{P}\right) \tag{11}$$

Considering the relationship between surface molecular density and the SFG signal [N is proportional to the square root of the relevant SFG signal intensity (eq 9)], eq 11 becomes

$$\frac{1}{\sqrt{I_{SF}}} = \frac{1}{\sqrt{I_{SF,max}}} + \frac{1}{K(T)\sqrt{I_{SF,max}}}\left(\frac{1}{P}\right) \tag{12}$$

The relationship between the inverse square root of the SFG intensity and the inverse methanol pressure is shown in Figure 12.

Upon fitting the linear portion of the data in Figure 12, the chemisorption constant at room temperature, $K(T = 298\ K)$, is calculated to be $(2.13 \pm 0.14) \times 10^3$. This value reflects partitioning of the adsorbates between phases at the sorbent−sorbate interface. The corresponding adsorption free energy, ΔG, is -19 ± 1.3 kJ mol^{-1}. This value is comparable to the reported free energy change of TiO_2 upon adsorption of acetone vapor, which is in the range of -10 to -19 kJ mol^{-1} obtained by Sun and Berg[60] using inverse gas chromatography. The negative free energy indicates a spontaneous process for gaseous methanol adsorption on the TiO_2 surface to form methoxy. The heat of

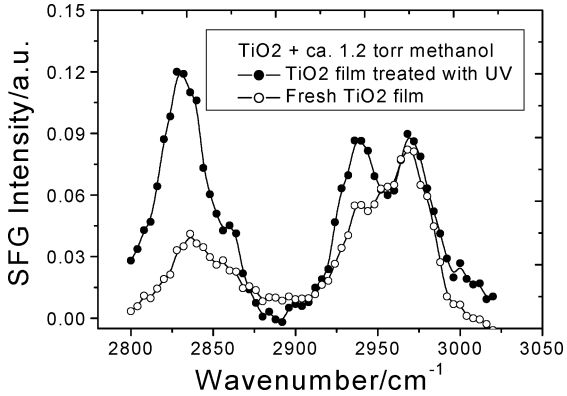

Figure 13. Effect of UV pretreatment of the TiO_2 film on the adsorption of methanol.

adsorption for methoxy on TiO_2 surface has been reported to be ca. 77 kJ mol^{-1} based on a "first principles" calculation.[33] The chemisorption entropy of methoxy is thereby derived to be ca. -45 J mol^{-1} K^{-1}. The negative entropy change, ΔS, is consistent with the nature of the adsorption process. Upon adsorption, the gaseous methanol is confined to a two-dimensional surface from a three-dimensional space, and consequently, the order of the system is increased.

Adsorption isotherms are often obtained by a conventional volumetric adsorption apparatus.[48] In this case, the isotherm is a convolution of all adsorption modes. If the adsorption contains more than one mode, it is hard to discriminate among them with this approach. In contrast, the chemisorption isotherm of methoxy on the surface of TiO_2 can be determined by SFG, although physisorption of methanol coexists in the system. The surface active sites for different films can be evaluated by comparing the SFG intensities of methoxy at pressures less than the inflection point pressure in the adsorption isotherm. The stronger the SFG signal of methoxy observed, the more active sites are present on the surface.

3.4.2. UV Treatment of the Surface. TiO_2 is well-known for its photocatalytic activity. An evaluation of the effect of UV irradiation on the surface sites is of general interest. Figure 13 shows two SFG spectra of methanol in contact with the TiO_2 film: one without UV irradiation and the second following UV pretreatment. Note that the SFG signal from methoxy is more sensitive to the surface treatment than is molecular methanol.

Methoxy formation is substantially enhanced by UV pretreatment. This agrees well with recent findings of surface wettability conversion with UV irradiation on TiO_2.[9,13,61] A stoichiometric TiO_2 surface contains different types of Ti, e.g., 5- and 6-fold coordinated, and different O sites such as in-plane and bridging, or 3- and 2-fold coordinated atoms. In practice, there are also defects or vacancies on the surface. From a thermodynamic point of view, the surface sites relating to unsaturated atoms are energetically unstable and therefore, are the surface active sites. In addition, TiO_2 has an amphoteric character. The unsaturated titanium surface atoms work as Lewis acids while oxygen sites act as Lewis bases. Under ambient condition where water vapor is present, the processes depicted in eqs 13 and 14 are expected to occur.

Thus, a freshly prepared TiO_2 film surface is saturated with hydroxyl groups, referred to as hydroxylation. Hydroxylation polarizes the surface atoms and facilitates adsorption. It is important to keep in mind that, apart from dissociative adsorption, water can also be molecularly adsorbed on the bare surface or be physisorbed through hydrogen bonding on the hydroxylated surface. Discussions of adsorption of water on TiO_2 can be found in the literature.[13,34,62,63]

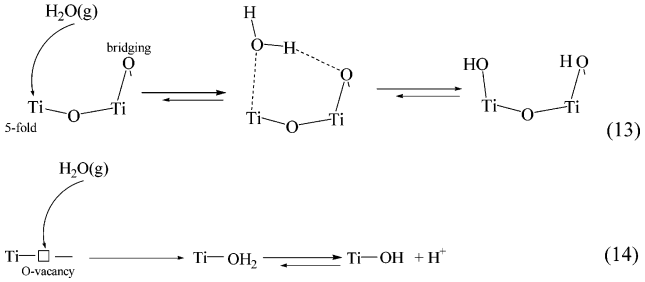

When methanol approaches the TiO_2 surface, it reacts with the surface OH groups, resulting in methoxy chemisorbed to the surface:

$$\text{Ti-OH} + \text{CH}_3\text{OH} \rightarrow \text{Ti-OCH}_3 + \text{H}_2\text{O} \quad (15)$$

This is supported by the observation that the SFG signal from the surface OH groups of TiO_2 is damped in the presence of methanol.[40] The coupling effect between σ-bond electrons in methoxy ($-OCH_3$) and the d orbitals of Ti weakens the C−H bond strength of the $-CH_3$ group, resulting in a red shift of the vibrational resonance as shown in Figure 5.

Upon UV irradiation, surface-adsorbed hydrocarbons on the TiO_2 film are catalytically oxidized.[39] In addition, UV irradiation generates more surface oxygen vacancy sites:[1,64]

$$\text{TiO}_2 + h\nu \rightarrow \text{h}^+ + \text{e}^- \quad (16)$$

$$\text{Ti-O}^{2-} + \text{h}^+ \rightarrow \text{Ti-O}^- \quad (17)$$

$$\text{Ti-O}^- + \text{h}^+ \rightarrow {}^1/_2\text{O}_2 + \text{Ti-}\square\text{- (oxygen vacancy)} \quad (18)$$

$$\text{Ti}^{4+} + \text{e}^- \rightarrow \text{Ti}^{3+}\ \text{(surface trapped)} \quad (19)$$

The photogenerated oxygen vacancy sites favor water adsorption, and hence, more surface OH groups are produced. UV enhancement of the OH density on the surface has been confirmed in previous studies.[13,40] Both results of UV treatment stated above increase chemisorption of methanol on the TiO_2 surface. Thus, an enhanced methoxy signal is observed. UV irradiation not only cleans the TiO_2 surface but also increases surface activity. This conclusion is directly relevant to the reversible wetting phenomenon as well as to practical applications of TiO_2. For example, solar cells assembled from UV-pretreated TiO_2 have been found to produce an enhanced photocurrent response.[65]

Adsorption of methoxy on TiO_2 is sensitive to the surface treatment by UV (Figure 13) so the adsorption of methoxy is related to surface active sites. Theoretical simulations show that methoxy prefers to adsorb on 5-fold coordinated titanium atom sites.[33] Chemisorption of methoxy is directly related to surface OH coordinated to unsaturated or oxygen vacancy-related Ti atoms on the surface; hence, methoxy serves as an indicator of surface active sites. Thus, SFG can follow surface changes by monitoring changes in the methoxy signal.

In contrast to methoxy generation, adsorption of molecular methanol is relatively insensitive to the surface treatment (Figure 13). Molecular methanol can adsorb by an electrostatic effect or by displacement of physisorbed water on the surface. Static secondary ion mass spectroscopy (SSIMS) and TPD studies show that methanol molecularly adsorbs at nonvacancy sites.[66] Nonvacancy adsorption is consistent with peaks due to molecular methanol being insensitive to UV irradiation of the surface.

4. Summary

The adsorption of methanol on a nanoparticulate anatase TiO_2 film surface has been studied by using SFG. The SFG signal

variation with methanol pressure and with surface temperature demonstrates that there are two types of surface adsorption: molecular physisorption and dissociative chemisorption. Molecular methanol is more labile than methoxy. Chemisorption occurs at low temperature ($\ll -20$ °C), indicating a barrierless process. The Langmuir constant for the chemisorption is $(2.13 \pm 0.14) \times 10^3$ and the corresponding adsorption free energy, ΔG, is -19 ± 1.3 kJ mol^{-1}.

On the TiO_2 surface, the polarization combination *ssp* has significant intensity from all four primary SFG resonances of methanol and methoxy, while *sps* is more sensitive to methoxy resonances and *ppp* is more sensitive to the resonances of molecular methanol. Evaluation of the SFG signals with different polarization combinations for the symmetric and antisymmetric modes indicates that methoxy adsorbs on the surface more perpendicularly than molecular methanol.

The SFG signal of methoxy is more sensitive to surface changes than that of molecular methanol: UV pretreatment of the TiO_2 film significantly enhances generation of methoxy. This indicates that methoxy is the result of adsorption at Ti sites that are unsaturated or oxygen vacancy-related. Enhancement of the SFG signal from methoxy following UV treatment agrees well with the recent finding of wettability conversion of TiO_2 by UV irradiation. The SFG of methoxy on the TiO_2 provides an effective molecular probe of surface changes.

Acknowledgment. C.-y.W. thanks Professor Steve Baldelli (at University of Houston) for valuable discussion. Financial support by the National Science Foundation (CHE-9816380) is gratefully acknowledged.

References and Notes

(1) Hoffmann, M. R.; Martin, S. T.; Choi, W. Y.; Bahnemann, D. W. *Chem. Rev.* **1995**, *95*, 69−96.
(2) Wamer, W. G.; Yin, J. J.; Wei, R. R. *Free Radicals Biol. Med.* **1997**, *23*, 851−858.
(3) Oregan, B.; Gratzel, M. *Nature* **1991**, *353*, 737−740.
(4) Wang, R.; Hashimoto, K.; Fujishima, A.; Chikuni, M.; Kojima, E.; Kitamura, A.; Shimohigoshi, M.; Watanabe, T. *Nature* **1997**, *388*, 431−432.
(5) Wolfrum, E. J.; Huang, J.; Blake, D. M.; Maness, P. C.; Huang, Z.; Fiest, J.; Jacoby, W. A. *Environ. Sci. Technol.* **2002**, *36*, 3412−3419.
(6) Ohshima, K.; Tsuto, K.; Okuyama, K.; Tohge, N. *Kag. Kog. Ronbunshu* **1997**, *23*, 237−242.
(7) Johnson, R. W.; Thiele, E. S.; French, R. H. *Tappi J.* **1997**, *80*, 233−239.
(8) Wang, R.; Hashimoto, K.; Fujishima, A.; Chikuni, M.; Kojima, E.; Kitamura, A.; Shimohigoshi, M.; Watanabe, T. *Adv. Mater.* **1998**, *10*, 135−138.
(9) Wang, R.; Sakai, N.; Fujishima, A.; Watanabe, T.; Hashimoto, K. *J. Phys. Chem. B* **1999**, *103*, 2188−2194.
(10) Erdem, B.; Hunsicker, R. A.; Simmons, G. W.; Sudol, E. D.; Dimonie, V. L.; El-Aasser, M. S. *Langmuir* **2001**, *17*, 2664−2669.
(11) McCafferty, E.; Wightman, J. P. *Surf. Interface Anal.* **1998**, *26*, 549−564.
(12) Fukui, K.-I.; Iwasawa, Y. *Surf. Sci.* **2000**, *464*, L719−L726.
(13) Nakamura, R.; Ueda, K.; Sato, S. *Langmuir* **2001**, *17*, 2298−2300.
(14) Liao, L.-F.; Wu, W.-C.; Chuang, C.-C.; Lin, J.-L. *J. Phys. Chem. B* **2001**, *105*, 5928−5934.
(15) Brazdil, J. F.; Yeager, E. B. *J. Phys. Chem.* **1981**, *85*, 1005−1014.
(16) Gutierrez-Alejandre, A.; Ramirez, J.; Busca, G. *Langmuir* **1998**, *14*, 630−639.
(17) Henderson, M. A. *Surf. Sci.* **1996**, *355*, 151−166.
(18) Henderson, M. A. *J. Phys. Chem. B* **1997**, *101*, 221−229.
(19) Shen, Y. R. *Nature* **1989**, *337*, 519−525.
(20) Shen, Y. R. *Solid State Commun.* **1998**, *108*, 399−406.
(21) Shultz, M. J.; Baldelli, S.; Schnitzer, C.; Simonelli, D. *J. Phys. Chem. B* **2002**, *106*, 5313−5324.
(22) Shultz, M. J.; Schnitzer, C.; Simonelli, D.; Baldelli, S. *Int. Rev. Phys. Chem.* **2000**, *19*, 123−153.
(23) Richmond, G. L. *Annu. Rev. Phys. Chem.* **2001**, *52*, 357−389.
(24) Richmond, G. L. *Chem. Rev.* **2002**, *102*, 2693−2724.
(25) Ma, G.; Allen, H. C. *J. Am. Chem. Soc.* **2002**, *124*, 9374−9375.
(26) Chen, Z.; Ward, R.; Tian, Y.; Baldelli, S.; Opdahl, A.; Shen, Y. R.; Somorjai, G. A. *J. Am. Chem. Soc.* **2000**, *122*, 10615−10620.
(27) Chen, Q.; Zhang, D.; Somorjai, G.; Bertozzi, C. R. *J. Am. Chem. Soc.* **1999**, *121*, 446−447.
(28) Kim, J.; Cremer, P. S. *J. Am. Chem. Soc.* **2000**, *122*, 12371−12372.
(29) Moruzzi, G. *Microwave, infrared, and laser transitions of methanol: atlas of assigned lines from 0 to 1258 cm*$^{-1}$; CRC Press: Boca Raton, FL, 1995.
(30) Onishi, H.; Aruga, T.; Egawa, C.; Iwasawa, Y. *Surf. Sci.* **1988**, *193*, 33−46.
(31) Ramis, G.; Busca, G.; Lorenzelli, V. *J. Chem. Soc., Faraday Trans. 1* **1987**, *83*, 1591−1599.
(32) Kim, K. S.; Barteau, M. A. *Surf. Sci.* **1989**, *223*, 13−32.
(33) Bates, S. P.; Gillan, M. J.; Kresse, G. *J. Phys. Chem. B* **1998**, *102*, 2017−2026.
(34) Herman, G. S.; Dohnalek, Z.; Ruzycki, N.; Diebold, U. *J. Phys. Chem. B* **2003**, *107*, 2788−2795.
(35) Wang, C. Y.; Rabani, J.; Bahnemann, D. W.; Dohrmann, J. K. *J. Photochem. Photobiol. A: Chem.* **2002**, *148*, 169−176.
(36) Wang, C. Y.; Bahnemann, D. W.; Dohrmann, J. K. *Chem. Commun.* **2000**, 1539−1540.
(37) Sun, L. Z.; Bolton, J. R. *J. Phys. Chem.* **1996**, *100*, 4127−4134.
(38) Bell, G. R.; Bain, C. D.; Ward, R. N. *J. Chem. Soc., Faraday Trans.* **1996**, *92*, 515−523.
(39) Guyot-Sionnest, P.; Superfine, R.; Hunt, J. H.; Shen, Y. R. *Chem. Phys. Lett.* **1988**, *144*, 1−5.
(40) Wang, C.-Y.; Groenzin, H.; Shultz, M. J. *Langmuir* **2003**, *19*, 7330−7334.
(41) Brus, L. *J. Phys. Chem.* **1986**, *90*, 2555−2560.
(42) Kormann, C.; Bahnemann, D. W.; Hoffmann, M. R. *J. Phys. Chem.* **1988**, *92*, 5196−5201.
(43) Serpone, N.; Lawless, D.; Khairutdinov, R. *J. Phys. Chem.* **1995**, *99*, 16646−16654.
(44) Stanners, C. D.; Du, Q.; Chin, R. P.; Cremer, P.; Somorjai, G. A.; Shen, Y. R. *Chem. Phys. Lett.* **1995**, *232*, 407−413.
(45) Superfine, R.; Huang, J. Y.; Shen, Y. R. *Phys. Rev. Lett.* **1991**, *66*, 1066−1069.
(46) Wolfrum, K.; Graener, H.; Laubereau, A. *Chem. Phys. Lett.* **1993**, *213*, 41−46.
(47) Wu, W. C.; Chuang, C. C.; Lin, J. L. *J. Phys. Chem. B* **2000**, *104*, 8719−8724.
(48) Suda, Y.; Morimoto, T.; Nagao, M. *Langmuir* **1987**, *3*, 99−104.
(49) Wang, J.; Chen, C. Y.; Buck, S. M.; Chen, Z. *J. Phys. Chem. B* **2001**, *105*, 12118−12125.
(50) Zhuang, X.; Miranda, P. B.; Kim, D.; Shen, Y. R. *Phys. Rev. B* **1999**, *59*, 12632−12640.
(51) Watanabe, N.; Yamamoto, H.; Wada, A.; Domen, K.; Hirose, C.; Ohtake, T.; Mino, N. *Spectrochim. Acta A: Mol. Biomol. Spectrosc.* **1994**, *50*, 1529−1537.
(52) Hirose, C.; Yamamoto, H.; Akamatsu, N.; Domen, K. *J. Phys. Chem.* **1993**, *97*, 10064−10069.
(53) Ferraro, J. R.; Nakamoto, K. *Introductory Raman Spectroscopy*; Academic Press: Boston, MA, 1994.
(54) Zhang, D.; Gutow, J.; Eisenthal, K. B. *J. Phys. Chem.* **1994**, *98*, 13729−13734.
(55) Wolfrum, K.; Laubereau, A. *Chem. Phys. Lett.* **1994**, *228*, 83−88.
(56) Colles, M. J.; Griffiths, J. E. *J. Chem. Phys.* **1972**, *56*, 3384−3391.
(57) Gough, K. M. *J. Chem. Phys.* **1989**, *91*, 2424−2432.
(58) Matsumoto, M.; Kataoka, Y. *J. Chem. Phys.* **1989**, *90*, 2398−2407.
(59) Adamson, A. W. *Physical chemistry of surfaces*, 5th ed.; Wiley: New York, 1990.
(60) Sun, C. H.; Berg, J. C. *J. Chromatogr. A* **2002**, *969*, 59−72.
(61) Sakai, N.; Fujishima, A.; Watanabe, T.; Hashimoto, K. *J. Phys. Chem. B* **2003**, *107*, 1028−1035.
(62) Bredow, T.; Jug, K. *Surf. Sci.* **1995**, *327*, 398−408.
(63) Smith, P. B.; Bernasek, S. L. *Surf. Sci.* **1987**, *188*, 241−254.
(64) Sun, R. D.; Nakajima, A.; Fujishima, A.; Watanabe, T.; Hashimoto, K. *J. Phys. Chem. B* **2001**, *105*, 1984−1990.
(65) Gregg, B. A.; Chen, S.-G.; Ferrere, S. *J. Phys. Chem. B* **2003**, *107*, 3019−3029.
(66) Henderson, M. A.; Otero-Tapia, S.; Castro, M. E. *Faraday Discuss.* **1999**, 313−329.